RESEARCH ON OPTIMAL CONTROL OF MINE-USED PERMANENT MAGNET DIRECT-DRIVE VARIABLE FREQUENCY INTEGRATED MACHINE BASED ON EXTENDED KALMAN FILTER

Sen WANG[1], Nan CHEN[2], Chong TANG[3], Jianmin DU[4], Zhanyang YU[5]

The vector control of the motor relies on the motor terminal voltage and stator current as important feedback signals. Conventional motor control systems obtain them by using mechanical sensors. However, such sensors are not conducive to smooth operation of mining motors. We have designed a control strategy based on the Extended Kalman Filter. We enhance the observation accuracy by modifying the noise matrices Q and R within the EKF. Simulation results demonstrate that the optimized EKF exhibits improvements in reducing convergence time and minimizing speed impact values.

Keywords: permanent magnet direct drive machine, extended Kalman filter, position-sensorless control, optimal control

1. Introduction

As the mining industry moves towards intelligent mining, researchers have developed a high-power, high-voltage variable frequency motor integrated drive system. This strategy combines the frequency converter and the motor more effectively. This fundamentally resolves the issue of poor coordination between the motor and the inverter switches. It enhances the safety and automation level of mining operations. It holds significant economic value in terms of reducing energy consumption by Wang L et al. (2020) and Kakihara M et al. (2020) .

By Gaolin L et al. (2017) and Gao W et al. (2021), they apply PI control to the vector control system. This achieves constant voltage-to-frequency ratio control for asynchronous motors without the need for speed sensors. However, due to the dependency of vector control on the motor, it has not led to improved control

[1] Associate Professor, School of Automation, Shenyang Institute of Engineering, China. e-mail: forest.king@qq.com
[2] Master, School of Automation, Shenyang Institute of Engineering, China. e-mail: 729767254@qq.com
[3] Lecturer, School of Automation, Shenyang Institute of Engineering, China. e-mail: 171833019@qq.com
[4] Lecturer, School of Electrical Engineering, shenyang University of Technology, China. e-mail: ddzhanyang@sina.com
[5] Lecturer, School of Electrical Engineering, shenyang University of Technology, China. e-mail: ddzhanyang@sina.com

accuracy. Chebaani M et al. (2018) was proposed early on to apply sensorless control technology to mining permanent magnet direct-drive variable frequency integrated machines. They adopted a high-frequency signal injection control strategy and achieved good control results.However, the injection of high-frequency signals still causes motor vibrations. The issue at hand has not been appropriately resolved. Demir et al. (2018) and Noori, O. B.et al. (2020) proposed the incorporation of extended Kalman filtering to estimate the position and velocity of the rotor.This strategy has demonstrated commendable stability in both motor unloaded and loaded conditions. However, they lack comparative simulations and have not achieved optimization outcomes. Lingrui L.et al. (2017) and Aleksandr, S.et al. (2020) proposed manipulating the rotor resistance of the motor to emulate its operating conditions. They utilized this variation to evaluate the stability of the EKF-based control strategy. The simulation results indicated that the system was not sensitive to variations in motor parameters. Its value still maintained a high level of robustness. However, they did not conduct any research on the optimization aspects of the EKF. Khadar, S.et al. (2021), Khanesaret al. (2022) and Emrah, Z.et al. (2018) established an EKF-based direct torque control system. They obtained the speed and flux waveforms at low speeds. However, they did not set up a control group for comparison when assigning values to the covariance matrix in the control strategy. We will pay particular attention to addressing this issue.

We adopt an integrated design approach, combining the inverter with a permanent magnet synchronous motor. This fact breaks the disadvantages of the conventional separate design of motors and frequency converters, followed by integration in the later stages. Due to its smaller size and limited space, we have higher requirements for the control strategy. We are studying the application of the mine-used permanent magnet integrated frequency converter in low-speed direct drive scraper conveyors. Its rated speed is 80 r/min. So, the design emphasis of the control system should be placed on the low-speed range. Its speed control range is within the range of 0-100 r/min. We conducted a study on the selection of covariance matrix initial values in the algorithm by establishing a simulation model of the EKF. From this study, we obtained the patterns of variation and were able to construct an optimized EKF accordingly.

2. Motor control principle based on Extended Kalman Filter

Currently, EKF is widely used in motor observation applications. It includes observations of parameters such as speed, position, or angle measurements of the motor. EKF extends the Kalman filter by Jacobian matrix formulation of the state transition matrix and the observation matrix. This allows for local processing of nonlinear systems using Taylor expansion, approaching the optimal estimation value. It can utilize the observed results to perform system adjustment and tuning.

And it filters out the influence of uncertainties, making the final result tend towards linearization.

The control system of the permanent magnet direct drive inverter is nonlinear in terms of output. Therefore, EKF algorithm will have a good control performance. By discretizing the mathematical model of the motor, we obtain:

$$\begin{cases} u_\alpha = Ri_\alpha + L_s \dfrac{di_\alpha}{dt} - \omega_e \psi_f \sin\theta_e \\ u_\beta = Ri_\beta + L_s \dfrac{di_\beta}{dt} - \omega_e \psi_f \sin\theta_e \end{cases} \tag{1}$$

Where i_α, i_β are the motor α and β axis current; u_α, u_β are the motor α and β axis voltage; ω_e, θ_e are rotor electric angular velocity and rotor position angle; R, L_s are motor stator phase resistance and phase inductance; ψ_f is permanent magnet flux linkage.

The control system of the all-in-one machine is nonlinear for the output, so the EFK algorithm will have a good control performance. To begin with, we take into account formula (2).

$$\begin{cases} \dfrac{d\omega_e}{dt} = 0 \\ \dfrac{d\theta_e}{dt} = \omega_e \end{cases} \tag{2}$$

We can derive the following formula describing the state.

$$\frac{d}{dt}x = f(x) + \begin{bmatrix} \dfrac{1}{L_s} & 0 \\ 0 & \dfrac{1}{L_s} \\ 0 & 0 \\ 0 & 0 \end{bmatrix} u \tag{3}$$

$$y = \begin{bmatrix} 1 & 0 & 0 & 0 \\ 0 & 1 & 0 & 0 \end{bmatrix} x \tag{4}$$

Among them.

$$x = \begin{bmatrix} i_\alpha \\ i_\beta \\ \omega_e \\ \theta_e \end{bmatrix}, u = \begin{bmatrix} u_\alpha \\ u_\beta \end{bmatrix}, y = \begin{bmatrix} i_\alpha \\ i_\beta \end{bmatrix} \tag{5}$$

Where x is composed of α, β axis current, rotor speed and position; u is composed of α, β axis voltage; y is composed of α, β axis current.

$$f(x)=\begin{bmatrix} -\frac{R}{L_s}i_\alpha+\omega_e\frac{\psi_f}{L_s}\sin\theta_e \\ -\frac{R}{L_s}i_\beta+\omega_e\frac{\psi_f}{L_s}\sin\theta_e \\ 0 \\ \theta_e \end{bmatrix} \tag{6}$$

Where $f(x)$ is composed of the motor stator equation and the rotor position.

By discretizing the mathematical model of the all-in-one machine, formula (7) and (8) are obtained.

$$x(k+1)=f[x(k)]+\begin{bmatrix} \frac{1}{L_s} & 0 & 0 & 0 \\ 0 & \frac{1}{L_s} & 0 & 0 \end{bmatrix}^T u(k)+V(k) \tag{7}$$

$$y(k)=\begin{bmatrix} 1 & 0 & 0 & 0 \\ 0 & 1 & 0 & 0 \end{bmatrix}x(k)+W(k) \tag{8}$$

Where $V(k)$ is system noise; $W(k)$ is measuring noise.

The noise vectors V and W are not directly involved in the iterative process of EKF. The EKF relies primarily on the covariance matrix Q for V and the covariance matrix R for W. The noise matrices Q and R are defined as follows:

$$\begin{cases} \cos(V)=E\left(VV^T\right)=Q \\ \cos(W)=E\left(WW^T\right)=R \end{cases} \tag{9}$$

The state estimation of the EKF can be roughly divided into two phases. The initial phase corresponds to the prediction stage. The second phase involves the correction stage.

First, the state vector is predicted. The state vector at time step (k+1) is predicted based on input $u(k)$ and the previous state estimate $x(k)$.

$$\tilde{x}(k+1)=\hat{x}(k)+T_s\left[f\left(\tilde{x}(k)\right)+B(k)u(k)\right] \tag{10}$$

In the equation, T_s represents the state sampling period. '^' represents the state sampling period. '~' represents the state prediction value.

To calculate the corresponding output $y(k+1)$ for this prediction, the process involves:

$$\tilde{y}(k+1)=C\tilde{x}(k+1) \tag{11}$$

To calculate the error covariance matrix, the process involves:

$$\tilde{p}(k+1)=\hat{p}(k)+T_s\left[F(k)\hat{p}(k)+\hat{p}(k)F^T(k)\right]+Q \tag{12}$$

In the formula, the variables are as follows:

$$F(k)=\frac{\partial f(x)}{\partial x}\Big|_{x=\hat{x}(k)} \tag{13}$$

The final prediction result is given by:

$$F(k)=\begin{bmatrix} -\frac{R}{L_s} & 0 & \frac{\psi_f}{L_s}\sin\hat{\theta}_e(k) & \hat{\omega}_e(k)\frac{\psi_f}{L_s}\cos\hat{\theta}_e(k) \\ 0 & -\frac{R}{L_s} & -\frac{\psi_f}{L_s}\cos\hat{\theta}_e(k) & \hat{\omega}_e(k)\frac{\psi_f}{L_s}\sin\hat{\theta}_e(k) \\ 0 & 0 & 0 & 0 \\ 0 & 0 & 1 & 0 \end{bmatrix} \tag{14}$$

To calculate the gain matrix $K(k+1)$ for EKF, the process involves:

$$K(k+1)=\tilde{p}(k+1)C^T\left[C\tilde{p}(k+1)C^T+R\right]^{-1} \tag{15}$$

By performing the feedback correction on the predicted state vector $x(k+1)$, we obtain the optimized state estimate $x(k+1)$. The process involves:

$$\hat{x}(k+1)=\tilde{x}(k+1)+K(k+1)\left[y(k+1)-\tilde{y}(k+1)\right] \tag{16}$$

In order to prepare for the next estimation, we need to pre-calculate the estimation error covariance matrix. The process involves:

$$\hat{p}(k+1)=\tilde{p}(k+1)=K(k+1)C\tilde{p}(k+1) \tag{17}$$

Can be seen from the formula (14), the permanent magnet variable frequency direct drive integrated machine system is a 4th-order nonlinear system. It takes stator flux, motor speed, and position as state variables. It takes the voltage in the α-β coordinate system as the system input. It takes the current as the output. The entire system is linear with respect to the input, but nonlinear with respect to the output. Based on this, it can be seen that EKF is applicable to the field-oriented control system of permanent magnet variable frequency direct drive integrated machines without position vectors. The control structure of the system is shown in Figure 1.

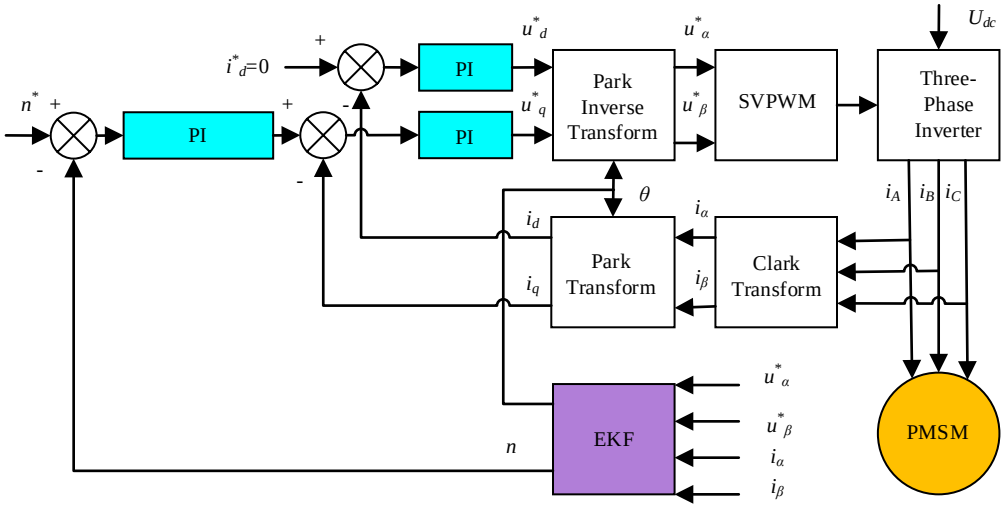

Fig. 1. System control structure diagram based on extended Kalman filter

3. Extended Kalman filter optimization control

We selected a 400kW mining-grade permanent magnet direct drive variable frequency integrated machine as the research object. As shown in Table 1, the specific parameters of the permanent magnet direct drive variable frequency integrated machine are listed. The system simulation diagram is shown in Figure 2. The entire simulation control system mainly consists of the EKF algorithm module, PI speed loop, PI current loop, and space vector pulse width modulation module.The EKF module is established using the s-function. We set the motor rated speed at 80 r/min. And the simulation time is set to 0.5 seconds.

Table 1

Mining permanent magnet direct drive inverter integrated machine parameters

Parameter	Value
R_s/Ω	0.06532
P_n	30
L/H	0.0085
Ψ_f/Wb	0.175
$J/(kg \cdot m^2)$	0.0048

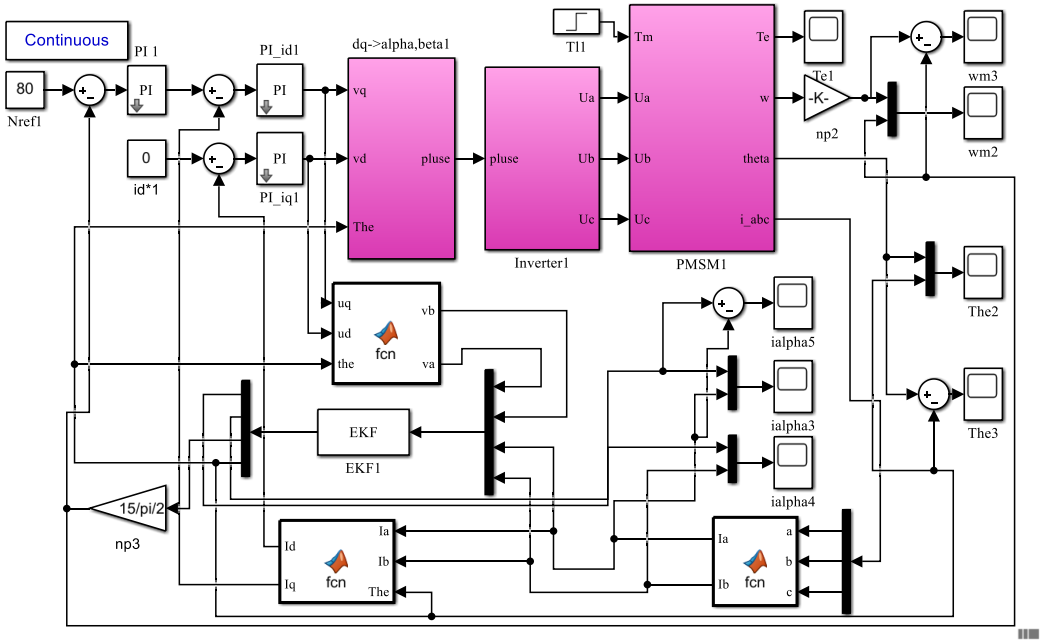

Fig. 2. Vector control system based on EFK

By Yin Z , Gao F , Zhang Y ,et al. (2019), the noise matrices Q and R will affect the filtering effect and speed estimation accuracy of EKF. Increasing the *Q*-value would intensify the noise in the EKF system. It amplifies the uncertainty of the EKF system model. The EKF prediction covariance and filter gain increase. Thus enhancing the observation error and responsiveness of the EKF. If the measurement noise *R*-value increases, this results in a reduction of the filter gain. The transient characteristics of the filter slow down, even to the extent of causing the filtering process to become unstable or divergent. In related EKF control systems, they often employ the following combinations:

$$\begin{aligned} Q &= diag(0.1 \quad 0.1 \quad 1 \quad 0.01) \\ R &= diag(0.01 \quad 0.01) \end{aligned} \tag{18}$$

The performance of EKF mainly includes observation accuracy and response speed. It is imperative for us to investigate the relationship between the noise matrix *QR* and the performance of EKF. We necessitate delving into the correlation between the noise matrices *Q* and *R*, and the performance of EKF. Sequentially altering the values of the noise matrices *Q* and *R*, we juxtapose the observational errors and response times of the system under varying conditions. In light of the values assigned to matrices *Q* and *R*, we configure ten distinct simulations for each. With regard to the values assigned to *Q*, we incrementally raise them from 0.02 to 0.2. With regard to the values assigned to *R*, we incrementally raise them from 0.002 to 0.02.

According to Figure 3, it is evident that as the value of *Q* increases, the overall observational error of the EKF exhibits an upward trend. Due to the fact that the noise matrix *Q* is a fourth-order matrix, the increase in observational error of the EKF is not linear. If we aim to enhance the observational accuracy of EKF, it is necessary to reduce the value of *Q*. The range of its increase is from 0.3985r/min to 0.6856r/min. Due to the significant improvement in optimization results with such a large range, it holds certain research value.

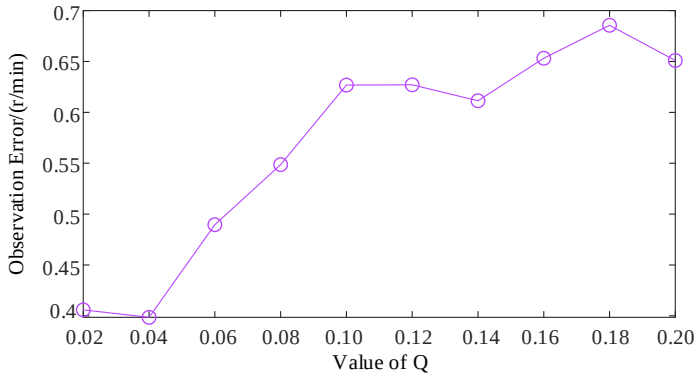

Fig. 3. The relationship between the value of Q and the observation error of EKF

According to Figure 4, it can be discerned that the augmentation of *Q* values induces a diminution in the response time of the EKF system. It shall elevate the responsiveness of the control system. By recalibrating the *Q* value, the response time was reduced from 0.1095s to 0.0742s. Such optimization proves advantageous for the motor control system. Hence, the adjustment of the *Q* value concurrently impacts the observational accuracy and responsiveness of the EKF.

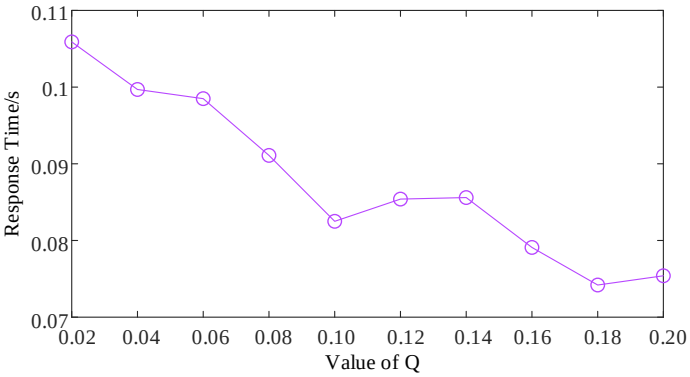

Fig. 4. The relationship between the value of Q and the response time of EKF

According to Figure 5, increasing the *R* value results in a reduction of observation error in the EKF, thereby enhancing its observational accuracy. By increasing the *R* value, the observation error decreased from 0.6654r/min to

0.5012r/min. Since R is a second-order matrix, we observe a pronounced decrease in the observation error trend.

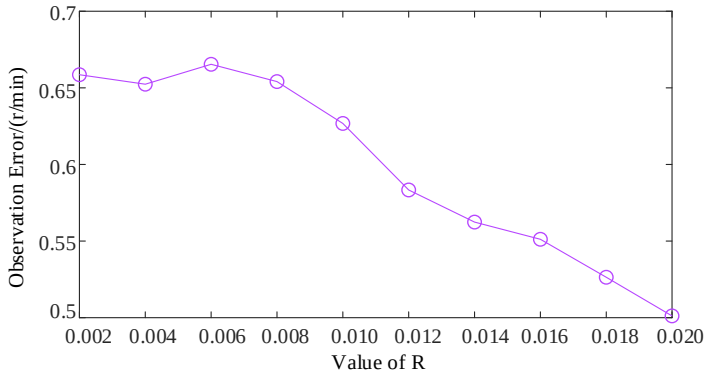

Fig. 5. The relationship between the value of R and the observation error of EKF

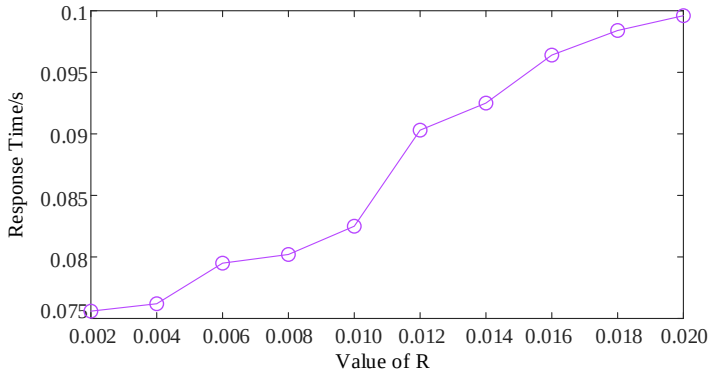

Fig. 6. The relationship between the value of R and the response time of EKF

According to Figure 6, with an increase in the *R* value, the response time of the EKF system also increases. By increasing the *R* value, the response time increased from 0.0756s to 0.0996s. This leads to a decrease in the system's response velocity, which hampers the stability of the control system. Consequently, adjusting the *R* value concurrently affects both the observation precision of EKF and the velocity influence. Moreover, the impact of the *R* value is contrary to that of the *Q* value.

Through the aforementioned analysis, we achieve a harmonious enhancement in both the observation precision and response velocity of EKF. The ultimate values for the selection of the noise matrices Q and R are as follows:

$$\begin{aligned} Q &= diag\begin{pmatrix} 0.12 & 0.12 & 0.8 & 0.008 \end{pmatrix} \\ R &= diag\begin{pmatrix} 0.012 & 0.008 \end{pmatrix} \end{aligned} \tag{19}$$

Subsequently, we incorporate this value into the control system of EKF. We validate the optimization effectiveness of EKF through the simulated model illustrated in Figure 2. The electric motor is initiated under no-load conditions, and

at 0.25 seconds, we apply a torque of 3 N·m to the motor. This procedure allows for the assessment of the control performance of EKF under various states. Figure 7 and Figure 8 represent the optimization effect of the observation accuracy in the EKF system. From Figure 7, it can be observed that the improved EKF significantly enhances its own speed observation accuracy in both the no-load and loaded states of the motor. From Figure 8, it can be concluded that in the loaded state of the motor, the improved EKF exhibits some improvement in the observed accuracy of the rotor position. Therefore, it can be inferred that the observation accuracy of the EKF is effectively improved.

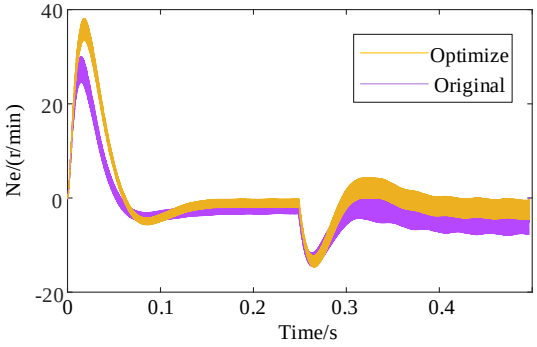

Fig. 7. Improving the speed observation error curve of EKF

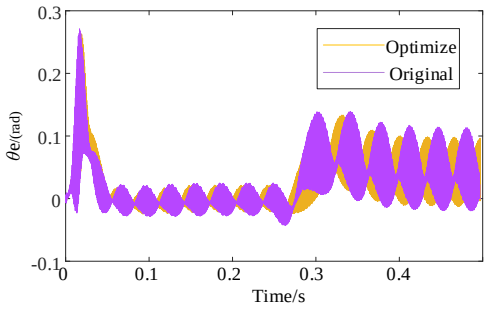

Fig. 8. Improving the rotor position observation error curve of EKF

Figure 9 and Figure 10 represent the optimization effect of the response speed in the EKF system. From Figure 9 and Figure 10, it can be observed that the improved EKF effectively reduces torque, speed overshoot, and improves the convergence speed of the curve when state transitions occur. Therefore, it can be concluded that the response speed of the EKF is effectively improved.

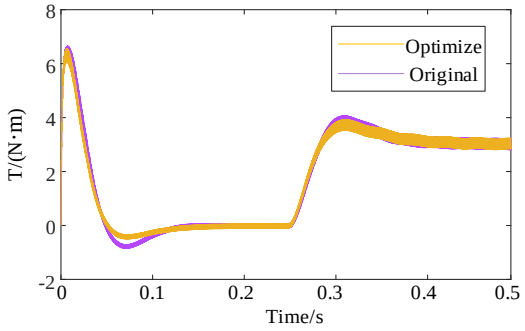

Fig. 9. Improving the torque response curve of EKF

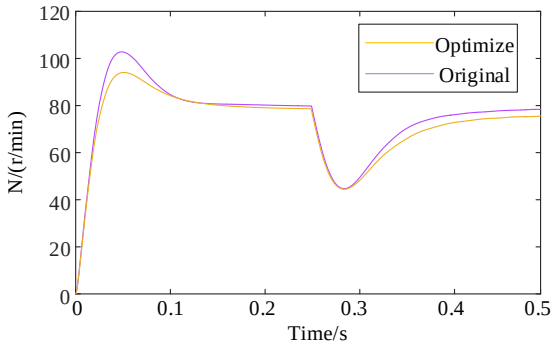

Fig. 10. Improving the speed response curve of EKF

4. Conclusion

Based on the findings, we propose the adoption of EKF for controlling mining permanent magnet variable frequency integrated machines. We have designed a vector control system based on EKF and conducted optimization research on it. We investigated the relationship between the initial values of the noise matrices *Q* and R within EKF and the performance of the EKF itself. By conducting comparative simulations, we obtained insights into the relationship between the noise matrices *Q* and *R* and the observation accuracy as well as response speed of the EKF. Based on the observed variations, we selected the optimal values for the noise matrices and applied them to the control system, resulting in an improved EKF control system. Through comparative simulations of parameters such as rotational speed and torque, we have demonstrated that the improved EKF exhibits higher observation accuracy and faster response speed. This finding holds significant reference value for the control research of mining permanent magnet variable frequency integrated machines.

Acknowledgment

The project is funded by Youth Project of Education Department of Liaoning Province.Funds:LJKQZ2021084.

The project is funded by Liaoning Provincial Department of Science and Technology - State Key Laboratory of Coal Mine Safety Technology Joint Opening Fund.Funds:2021-KF-13-02.

REFERENCES

[1]. *L. Wang L, J. Liu, X. Wang*, "Design and Implementation of Ansys-based Scraper Conveyor Permanent Magnet Frequency Conversion Integrated Machine." 2020 IEEE International Conference on Mechatronics and Automation, 2020.

[2]. *M. Kakihara, M. Takaki, M. Ohto*, "An Investigation of Servo Motor Structure for Sensorless Control Based on High-Frequency Injection Method." 2020 23rd International Conference on Electrical Machines and Systems, 2020.

[3]. *G. L. Wang, L. Yang*, "Comparative Investigation of Pseudorandom High-Frequency Signal Injection Schemes for Sensorless IPMSM Drives." IEEE Transactions on Power Electronics, 2017, pp. 2123-2129.

[4]. *W. Gao, G. Zhang, M. Hang*, "Sensorless Control Strategy of a Permanent Magnet Synchronous Motor Based on an Improved Sliding Mode Observer." World Electric Vehicle Journal, 2021, pp. 74-78.

[5]. *M. Chebaani, A Golea, M. T. Benchouia*, "Sensorless finite-state predictive torque control of induction motor fed by four-switch inverter using extended Kalman filter." Compel: International journal for computation and mathematics in electrical and electronic engineering, 2018, pp. 2006-2014.

[6]. *D. Ridvan, B. Murat*, "Novel hybrid estimator based on model reference adaptive system and extended Kalman filter for speed-sensorless induction motor control."Transactions of the Institute of Measurement and Control, 2018, pp. 3884-3888.

[7]. *O. B. Noori, M. O. Mustafa*, "Compressed Extended Kalman Filter for Sensorless Control of Asynchronous Motor." International Journal on Energy Conversion, 2020, pp. 200-204.

[8]. *L. R. Li, M. Z. Xu, X. D. Gao*, "Current Predictive Control Based on Extended Kalman Filter." Electric Machines & Control Application, 2017.

[9]. *S. Aleksandr, E. L. Kang*, "Sensorless Control of Hydrogen Pump Using Adaptive Unscented Kalman Filter." Journal of Harbin University of Science and Technology, 2020.

[10]. *S. Khadar, H. A. Abu-Rub, K. Abdellah, "*Sensorless Sliding Mode Control of Open-End Dual-Stator Induction Motor using Extended Kalman Filter." 18th IEEE International Multi-Conference on Systems, Signals & Devices, 2021.

[11]. *M. A. Khanesar, D. Branson*, "Robust Sliding Mode Fuzzy Control of Industrial Robots Using an Extended Kalman Filter Inverse Kinematic Solver." Energies, 2022.

[12]. *Z. Emrah*, "Adaptive Extended Kalman Filter for Speed-Sensorless Control of Induction Motors." IEEE Transactions on Energy Conversion, 2018, pp. 1-5.

[13]. *Z. Yin, F. Gao, Y. Zhang*, "A Review of Nonlinear Kalman Filter Appling to Sensorless Control for AC Motor Drives."Journal of Electrical Machinery and Systems of China Electrotechnical Society, 2019, pp. 12-16.